Comparing Intra- and Inter-individual Correlational Brain Connectivity from Functional and Structural Neuroimaging Data

Xin Di[1*], Bharat B. Biswal [1*], Alzheimer's Disease Neuroimaging Initiative[†]

1. Department of Biomedical Engineering, New Jersey Institute of Technology, Newark, NJ, 07102, USA

* Corresponding authors:

Xin Di, Ph.D.

604 Fenster Hall, University Height

Newark, NJ, 07102, USA

xin.di@njit.edu

Bharat B. Biswal, Ph.D.

607 Fenster Hall, University Height

Newark, NJ, 07102, USA

bbiswal@yahoo.com

† Data used in preparation of this article were obtained from the Alzheimer's Disease Neuroimaging Initiative (ADNI) database (adni.loni.usc.edu). As such, the investigators within the ADNI contributed to the design and implementation of ADNI and/or provided data but did not participate in analysis or writing of this report. A complete listing of ADNI investigators can be found at: http://adni.loni.usc.edu/wp-content/uploads/how_to_apply/ADNI_Acknowledgement_List.pdf

Abstract

Inferring brain connectivity from inter-individual correlations has been applied to various neuroimaging modalities, such as glucose metabolic activity measured by positron emission tomography (PET) and brain structures assessed using MRI. The variability that drives these inter-individual correlations is generally attributed to individual differences, potentially influenced by factors like genetics, life experiences, and biological sex. However, it remains unclear whether long-term within-individual effects, such as aging, and state-like effects also contribute to the correlated structures, and how intra-individual correlations are compared to inter-individual correlations. In this study, we analyzed longitudinal data spanning a wide age range, examining regional brain volumes using structural MRI, and regional brain functions using both regional homogeneity (ReHo) of resting-state functional MRI and glucose metabolic activity measured with Fludeoxyglucose (18F) FDG-PET. In a first dataset from a single individual scanned over 15 years, we found that intra-individual correlations in both ReHo and regional volumes resembled resting-state functional connectivity. In a second dataset, involving multiple longitudinal points and participants for FDG-PET and MRI, we replicated these findings, showing that both intra- and inter-individual correlations were strongly associated with resting-state functional connectivity. Correlations in functional measures (i.e., ReHo or FDG-PET) showed greater similarity with resting-state connectivity than structural measures. Moreover, matrices from the same modality showed higher similarity between the two datasets, indicating modality specific contributions. These results suggest that multiple factors may contribute to both inter- and intra-individual correlational measures of connectivity. Understanding or controlling for these factors could enhance the interpretability of the inter-individual connectivity measures.

Keywords: Brain connectivity; Covariance network; Functional Connectivity; Inter-individual; Molecular connectivity.

1. Backgrounds

Studies of brain connectivity are essential for advancing our understanding of functional interactions between brain regions and the organization of the whole brain. The development of neuroimaging techniques has provided an exciting opportunity to study brain function in humans in vivo. Early research frequently employed positron emission tomography (PET) to measure glucose metabolic activity (Phelps et al., 1981) and cerebral blood flow (Fox and Raichle, 1984). These studies primarily used inter-individual correlations of PET measures to quantify brain connectivity based on glucose metabolism (Horwitz et al., 1984; Metter et al., 1984) or cerebral blood flow (Zeki et al., 1991). However, due to the nature of PET measurements, which are static, these studies were generally limited to inter-individual correlations. While they often identified statistically significant connectivity patterns, the similarities between connectivity derived from PET measures and resting-state networks identified using functional MRI (fMRI) were relatively modest (Di et al., 2017; Di and Biswal, and Alzheimer's Disease Neu, 2012; Lizarraga et al., 2023).

Functional MRI (fMRI) has become a widely used tool for studying brain connectivity due to its superior spatial and temporal resolution (Biswal et al., 1995, 2010). Beyond capturing moment-to-moment dynamics, fMRI data can be summarized over brief periods, often during resting-state sessions, to derive measures such as the amplitude of low-frequency fluctuations (ALFF) (Zang et al., 2007) and regional homogeneity (ReHo) (Zang et al., 2004). These metrics have also been applied to examine inter-individual correlations of brain (Di et al., 2024a; Taylor et al., 2012; Zhang et al., 2011). Additionally, the flexibility of task designs in fMRI enables researchers to explore how task performance impacts inter-individual connectivity correlations. Studies indicate that while task conditions can induce slight changes in connectivity patterns, the overall connectivity structure tends to remain largely consistent across different tasks (Di et al., 2024a).

An intriguing extension of inter-individual correlation analysis is its application to brain structural data, which tends to reflect more trait-like characteristics associated with slow and long-term effects (He et al., 2007; Mechelli et al., 2005). Mechelli and colleagues were among the first to use a seed-based

approach to examine inter-individual correlations of regional brain volumes, discovering strong correlations between regions within the same functional brain systems (Mechelli et al., 2005). Building on this, He and colleagues constructed whole-brain networks based on inter-individual correlations of cortical thickness. Their findings demonstrated that these structural networks exhibit small-world properties, highlighting the efficiency and organization of the brain's structural connectivity (He et al., 2007).

Despite its growing popularity, questions remain about whether and to what extent inter-individual correlations reflect functional connectivity, which is traditionally assessed intra-individually, typically through resting-state fMRI. One approach to validate inter-individual correlational measures is to compare their similarity to other established connectivity measures, such as intra-subject moment-to-moment functional connectivity during rest or anatomical connectivity derived from white matter tracking. When using white matter tracking from diffusion-weighted imaging (DWI) as a reference, studies have found that inter-individual correlations of structural measures show limited similarity to white matter tracts (Gong et al., 2012; Lizarraga et al., 2023). In contrast, inter-individual correlations based on functional measures of glucose metabolic activity exhibit higher similarity with white matter connectivity (Lizarraga et al., 2023). A similar pattern emerges when comparing these measures to resting-state functional connectivity. Inter-individual structural correlations display limited similarity to resting-state functional connectivity (Alexander-Bloch et al., 2013b; Di et al., 2017). However, inter-individual correlations of functional measures, such as glucose metabolic activity, show greater alignment with resting-state connectivity patterns (Di et al., 2017).

A critical question remains regarding the factors driving inter-individual variability that lead to correlations in functional or structural brain measures. Do these correlations primarily reflect individual differences shaped by genetic factors or life experiences, or do intra-individual factors also play a role? For example, inter-individual correlation analyses often include large sample sizes spanning wide age ranges, prompting the question of whether age-related effects contribute significantly to these correlations

in brain structure. Exploring intra-individual correlations could provide valuable insights into the underlying causes of inter-individual variability.

In the context of functional data, such as glucose metabolism measured by FDG-PET, neural activity introduces an additional variable. This state-like factor may be influenced by participants' mental states at the time of measurement (Di et al., 2024a). Long-term brain activity, as reflected by metrics like FDG-PET or regional homogeneity (ReHo), typically persists over minutes to hours. However, it is unclear to what extent variability in this sustained activity contributes to the observed inter-individual correlations. Investigating intra-individual correlations in these slow functional activity patterns could shed light on the role of intra-individual variability in shaping inter-individual correlations.

In the current study, we examined correlations in brain structural and functional measures typically calculated in an inter-individual manner. We analyzed two unique datasets, allowing us to compute correlations both inter- and intra-individually, and compared the correlation structures derived from these two approaches. This comparison enabled us to estimate the contribution of intra-individual factors to the overall correlation structure. Specifically, the first dataset consists of a single individual scanned over 16 years (Duchesne et al., 2019), providing a unique opportunity to estimate gray matter and ReHo correlations intra-individually. The second dataset comes from the Alzheimer's Disease Neuroimaging Initiative (ADNI), focusing on healthy participants with more than five longitudinal FDG-PET scans. We calculated correlations in two ways: first, by calculating correlation matrices within each participant and then averaging these matrices across participants, which minimizes individual variability and focuses on intra-individual variability; and second, by calculating inter-individual correlations at each age point and averaging these matrices across ages, which focuses exclusively on inter-individual variability while controlling for factors such as age. Lastly, we compared correlation matrices between the two datasets and investigate whether different imaging modalities have their unique correlation structures.

2. Materials and Methods

2.1. Datasets

2.1.1. Simon dataset

The Simon dataset is available through the International Neuroimaging Data-Sharing Initiative (INDI) website (http://fcon_1000.projects.nitrc.org/indi/retro/SIMON.html). It includes data from a single heathy male who was scanned across 73 sessions over a 16-year period, from the age of 30 to 47. Figure 1A illustrates the distribution of these scanning sessions over time. In total, 73 MRI sessions are available, conducted using various scanners and parameters. For more details, refer to the original paper by (Duchesne et al., 2019). Our analysis focused on T1-weighted anatomical images and resting-state fMRI data, with 71 sessions providing T1-weighted images and 58 sessions containing resting-state fMRI data.

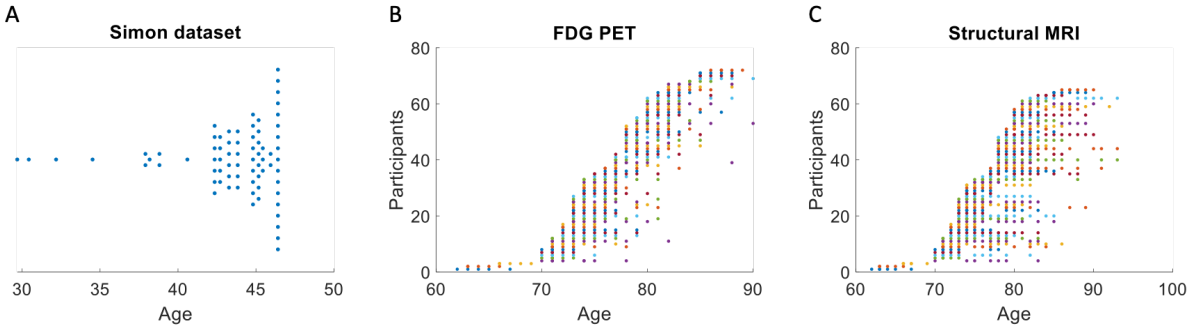

Figure 1 Illustration of scan sessions for the Simon dataset (A) and fludeoxyglucose-18 (FDG) positron emission tomography (PET) (B) and structural MRI (C) datasets from Alzheimer's Disease Neuroimaging Initiative (ADNI). For the Simon dataset, a single participant was scanned for 73 sessions over 16 years. Each dot represents one session. For the ADNI dataset, each row in y axis represents one participant, where each participant was scanned for multiple sessions.

2.1.2. ADNI dataset

The ADNI dataset was obtained from the project website (adni.loni.usc.edu). The ADNI was launched in 2003 as a public-private partnership, led by Principal Investigator Michael W. Weiner, MD. The primary goal of ADNI has been to test whether serial magnetic resonance imaging (MRI), positron emission tomography (PET), other biological markers, and clinical and neuropsychological assessment can be

combined to measure the progression of mild cognitive impairment (MCI) and early Alzheimer's disease (AD). For up-to-date information, see www.adni-info.org.

In this analysis, we only included data from healthy participants. All selected individuals showed no evidence of depression, mild cognitive impairment (MCI), or dementia, as indicated by Mini-Mental State Examination (MMSE) scores ranging from 24 to 30 and a Clinical Dementia Rating (CDR) of 0. We manually curated FDG-PET, MRI, and resting-state fMRI data for this study. For FDG-PET and MRI, we included participants with at least five sessions to ensure the calculation of reliable intra-individual correlations. For the resting-state fMRI data, we included only one session per individual and focused on the averaged correlation matrix across participants.

The data search began with FDG-PET, resulting in the inclusion of 72 participants (25 females) with a total of 432 PET scan sessions. The number of sessions per participant ranged from 5 to 9 (Figure 1B). The participants' average age at the first session was 75.8 years, with a range of 62 to 86 years. For each session, either a mean image was calculated, or a single representative image was used.

From the 72 participants with qualified PET data, we identified those with at least five sessions of structural MRI scans. A total of 65 participants met this criterion, with the number of MRI sessions ranging from 5 to 13. Figure 1C provides an overview of the session count and corresponding ages for these participants.

Finally, among the 65 participants with structural MRI data, 17 individuals also had resting-state fMRI scans available. For these participants, one session per individual was included, focusing on a single resting-state fMRI session per participant.

2.2. Data processing

Neuroimaging data processing and analysis were conducted using SPM12 (https://www.fil.ion.ucl.ac.uk/spm/) within MATLAB environment, following preprocessing and quality control procedures detailed in a prior study (Di and Biswal, 2023).

For the FDG-PET data, dynamic images (i.e., multiple images per session) were processed by realigning all images within a session to the first image, followed by generating a mean image for that

session. For static PET data, which contained only a single image per session, no realignment was required. Next, the mean images (or static images) from all sessions for each participant were realigned to the image from the first session. A cross-sessional mean image was then normalized directly to the PET template in SPM, aligned to the standard Montreal Neurological Institute (MNI) space. Normalization to MNI space was performed using consistent parameters across all images. Direct normalization was chosen over MRI-mediated normalization due to the sufficient spatial resolution of PET images and the methodological advantages of direct normalization (Calhoun et al., 2017). Finally, the normalized images were spatially smoothed using an 8 mm full-width at half-maximum (FWHM) Gaussian kernel, and each image was normalized by dividing its signal by the mean signal within an intracranial volume mask.

Each anatomical image was treated as independent data, segmented into gray matter, white matter, cerebrospinal fluid, and other tissues, and normalized to standard MNI space. Spatial normalization included modulation to ensure that the resulting gray matter images reflected gray matter volume (GMV). Quality control was performed by manually inspecting the anatomical images before and after segmentation. In the Simon dataset, one session was excluded due to segmentation failure, resulting in a total of 70 sessions being included in the final analysis.

For the fMRI data, the functional images were first realigned to the first image of each session. The mean functional image was then coregistered to the corresponding anatomical image. Next, the functional images were normalized to MNI space using the deformation field maps derived from the segmentation step and spatially smoothed with an 8 mm full-width at half-maximum (FWHM) Gaussian kernel. A voxel-wise general linear model was then applied to regress out head motion parameters and white matter/CSF signals. This model included 24 regressors based on Friston's head motion model, along with the first five principal components of signals from the white matter and cerebrospinal fluid. The residual images from this step were saved for further analysis.

For the Simon dataset, ReHo was calculated for each resting-state fMRI session using the REST toolbox (Song et al., 2011).

2.3. Brain parcellation

Cortical regions were defined using Schaefer's 100-region parcellation (Schaefer et al., 2018), while subcortical regions were identified based on the Automated Anatomical Labeling (AAL) atlas. The subcortical regions included the bilateral hippocampus, parahippocampus, amygdala, caudate, putamen, pallidum, and thalamus (Tzourio-Mazoyer et al., 2002).

For each participant and region, voxel values were averaged to compute measures of gray matter volume (GMV), FDG-PET, and regional homogeneity (ReHo), producing a 114-dimensional vector per participant. For resting-state fMRI data, the average time series for each region of interest (ROI) was extracted, resulting in a $114 \times n$ matrix, where n represents the number of time points, which varied across sessions and participants.

2.4. Calculation of intra- and inter-individual correlation matrices

In the Simon dataset, mean GMV values across 114 regions of interest (ROIs) for the 70 sessions were arranged into a 114 × 70 matrix. Pearson's correlation coefficients were then calculated to construct a within-individual GMV correlation matrix (114 × 114). Similarly, a ReHo correlation matrix was generated using ReHo maps from 58 sessions. For each of these 58 resting-state sessions, a resting-state connectivity matrix was also computed from the fMRI time series data. Finally, the correlation matrices from all sessions were averaged to produce a mean correlation matrix.

For the ADNI dataset, correlation matrices for FDG-PET or GMV were calculated across sessions for each participant. These matrices were then averaged across participants to produce a mean correlation matrix, referred to as the intra-individual correlation matrix. To calculate inter-individual correlations, participants' ages were controlled. Specifically, inter-individual correlations were computed at each integer age point where data from more than nine participants were available. This process was applied to participants aged between 70 and 89 years, and the resulting inter-individual correlation matrices were averaged to generate a mean correlation matrix, referred to as the inter-individual correlation matrix. Finally, for the fMRI data, resting-state functional connectivity matrices were calculated for each participant. These matrices were averaged across participants to obtain a mean connectivity matrix.

2.5. Statistical analysis

To investigate the associations among the correlation matrices, we extracted the upper diagonal of each matrix and converted it into a 6,441-dimensional vector (*114* x (*114* - *1*) / *2*). Given the potential non-Gaussian distribution of the correlation matrices, Spearman's rank correlation coefficient (ρ) was used to quantify the relationships among the matrices.

3. Results

3.1. Simon dataset

We first analyzed a multi-session dataset from a single individual spanning over 16 years. The averaged correlation matrix, shown in Figure 2A, reveals clear modular structures, evident as square-like patterns along the diagonal and additional squares representing left-right homotopic networks. Subsequently, we computed intra-individual correlations for regional brain volume (GMV) and ReHo across all available sessions. Both matrices display square-like patterns, although their spatial configurations differ. Notably, both intra-individual correlation matrices show moderate but significant correlations with the averaged resting-state time series correlation matrix (Spearman's correlation coefficients: $\rho_{GMV} = 0.29$; $\rho_{ReHo} = 0.39$).

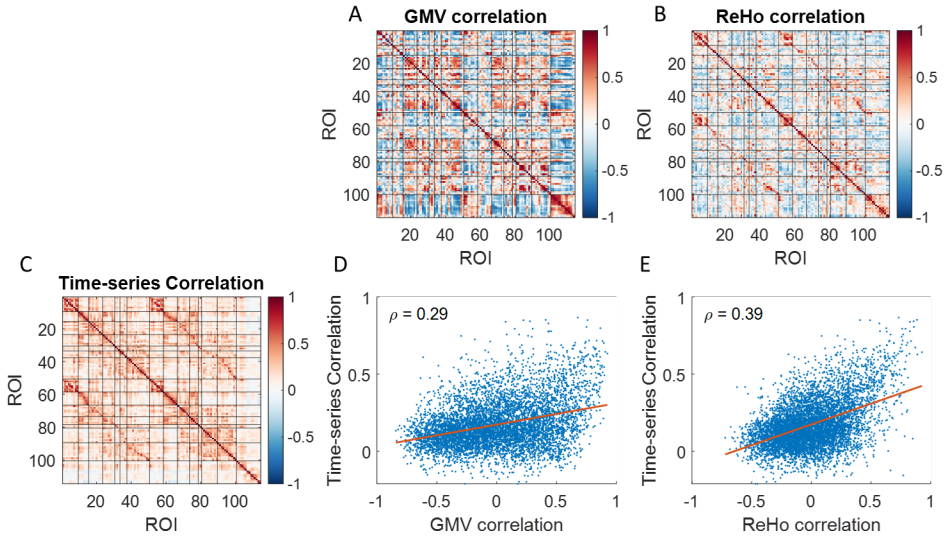

Figure 2 Correlations of regional brain volume (GMV) (A), regional homogeneity (ReHo) (B), and averaged correlations of resting-state time series (C) across 114 regions of interest (ROIs). D and E show the Spearman's correlations (ρ) between the time-series correlation matrix and GMV or ReHo correlations, respectively.

3.2. ADNI dataset

Next, we analyzed the ADNI dataset, where there were multiple participants, but each participant only have a few sessions. We calculated averaged resting-state time series correlation from the 17 participants (Figure 3A), which turned out to be very similar to those from the Simon dataset. We then calculated structural correlations both intra-individually and inter-individually. Both matrices demonstrated functional network structures along the diagonal and between left and right corresponding regions. Moreover, both correlation matrices were correlated with resting-state time series correlation (ρ_{intra} = 0.41; ρ_{inter} = 0.37), which were slightly higher than that in the Simon dataset (0.29).

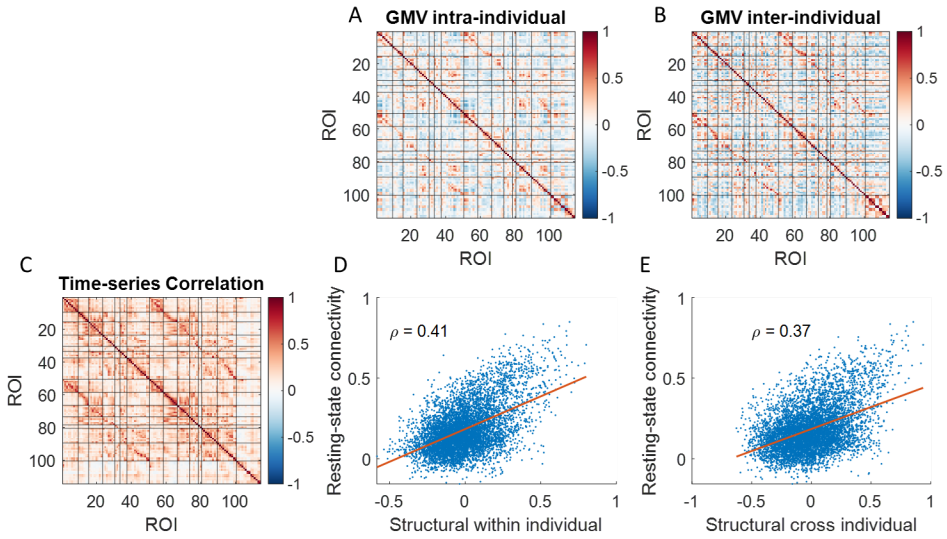

Figure 3 Correlations of regional brain volume (GMV) calculated intra-individually (A) and inter-individually (B), and averaged correlations of resting-state time series (C) across 114 regions o interests (ROIs). D and E show the Spearman's correlations (ρ) between the resting-state time series correlation matrix and GMV correlation matrices, respectively.

We next calculated correlations of glucose metabolic activity intra-individually and inter-individually, and correlated the correlation matrices with resting-state time series correlation (Figure 4). The correlations matrices of glucose metabolic activity showed more obvious functional network structures than those in structural correlations. And most importantly, the both correlation matrices showed strong correlations with resting-state time series correlation (ρ_{intra} = 0.71; ρ_{inter} = 0.64).

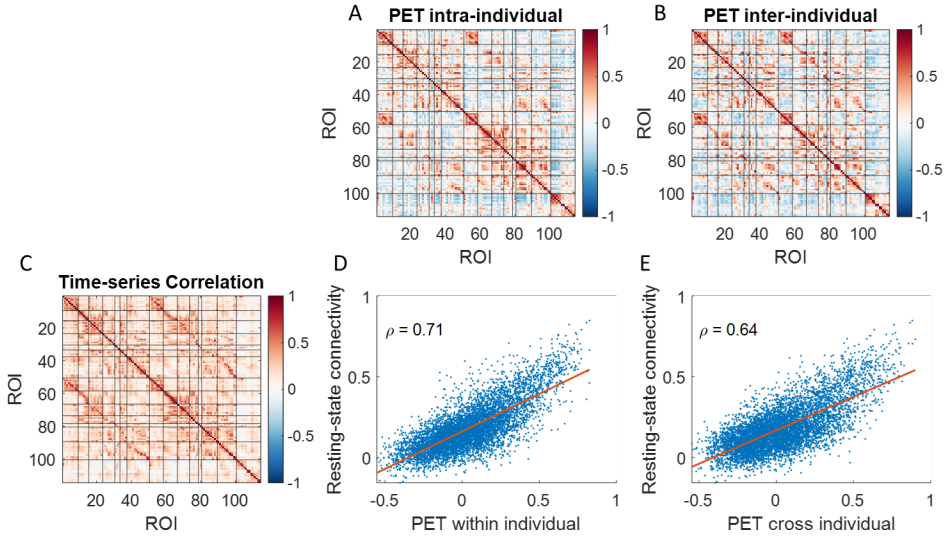

Figure 4 Correlations of regional brain glucose metabolism measured using positron emission tomography (PET) calculated intra-individually (A) and inter-individually (B), and averaged correlations of resting-state time series (C) across. D and E show the Spearman's correlations (ρ) between the resting-state time series correlation matrix with the two PET correlation matrices, respectiveely.

3.3. Relationships among all the matrices

Finally, we calculated the correlations among the correlation matrices (Figure 5A). Due to the large number of ROI pairs, all correlations were statistically significant. However, it is more meaningful to focus on the relative effects of these correlations rather than their statistical significance. Here, we emphasize the correlations between the matrices of the two datasets, where the highest correlations were observed between corresponding modalities (highlighted blue rectangle and diamond markers). For

instance, the strongest correlation with the mean time-series correlations in the Simon dataset was found with the time-series correlations in the ADNI dataset ($\rho = 0.67$). Similarly, the highest correlation with GMV correlations in the Simon dataset occurred with intra-individual GMV correlations in the ADNI dataset ($\rho = 0.46$), rather than inter-individual correlations. Notably, the highest correlation with ReHo correlations in the Simon dataset was observed with inter-individual PET correlations in the ADNI dataset ($\rho = 0.51$).

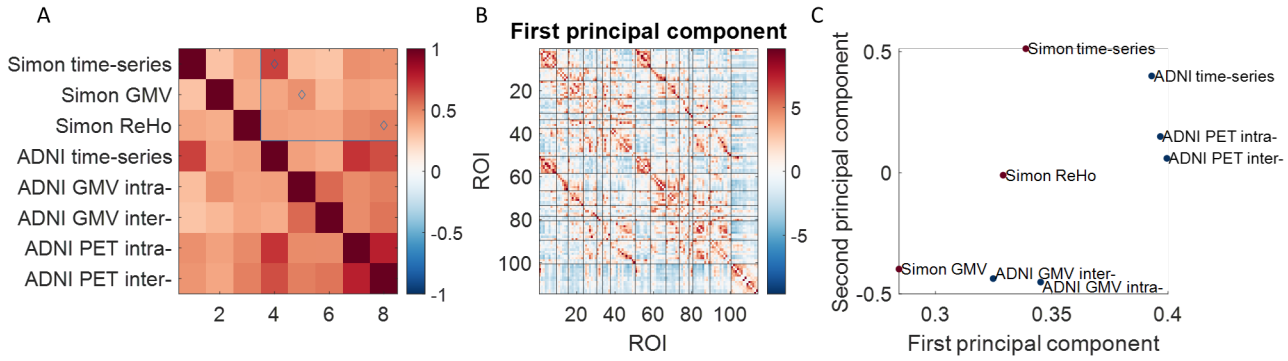

Figure 5 A. Spearman's correlation matrix among the correlation matrices. The blue rectangle and diamond markers highlight the effects of interest. B. The first principal component of the correlation matrices. C. Loadings of the correlation matrices on the first and second principal components. ADNI, Alzheimer's Disease Neuroimaging Initiative; GMV, gray matter volume; PET, positron emission tomography; ROI region of interest.

We then conducted a PCA on the eight correlation matrices, with the first principal component (PC) accounting for 59.0% of the variance (Figure 5B). Next, we visualized the loadings of the eight matrices on the first two PCs (Figure 5C). The matrices formed distinct clusters in the plot. For instance, the GMV correlation matrices were located at the bottom, while the time-series and PET correlation matrices clustered in the top-left corner.

4. Discussion

Using two unique datasets encompassing both intra- and inter-individual effects, the current analysis demonstrated how these effects contribute to correlation structures across brain regions. First, long-term structural brain changes revealed correlation patterns that were small but significantly associated with resting-state time-series correlations. Second, long-term functional activity, as measured by ReHo or glucose metabolism, exhibited stronger correlation structures and greater alignment with resting-state time-series correlations compared to structural measures. Finally, correlation matrices from the two datasets showed greater similarity within the same modality than between different modalities, suggesting that each modality provides distinct insights into interregional relationships.

This study analyzed a unique dataset from a single individual scanned over 16 years, revealing that intra-individual structural correlations were modestly associated with resting-state connectivity (ρ = 0.29), the lowest correlation observed among the analyses. This finding suggests that structural brain development and aging within an individual are partially constrained by the brain's functional organization. These results were further validated using the ADNI dataset, which, despite fewer longitudinal data points, showed a stronger correlation between intra-individual structural correlations and resting-state connectivity (ρ = 0.41). To our knowledge, this is the first study to demonstrate structural correlations within an individual, underscoring the influence of age as a single factor shaping these correlations.

Notably, inter-individual structural correlations, when controlling for chronological age, showed a similar association with resting-state connectivity (ρ = 0.37), indicating that individual differences contribute comparably. The variability that give rise to the inter-individual correlation may be related to genetics, life experience, and plasticity (Alexander-Bloch et al., 2013a; Evans, 2013). In previous studies of structural “covariance”, these factors could not be distinguished from development and aging effects. In fact, the current findings suggest that multiple factors could give rise to the correlation structure. This is also in line with studies showing that the structural “covariance” were modulated by factors such as age

(Vijayakumar et al., 2021). To enhance interpretability, researchers should consider restricting or controlling for such factors in their analyses.

To the best of our knowledge, this study is the first to demonstrate intra-individual correlations in long-term brain activity using either ReHo or FDG-PET measures. Notably, the correlations of ReHo and metabolic activity were generally higher than those of regional brain volumes. This suggests that summary measures of brain function may capture state-dependent activity, such as mood, thoughts, or other transient mental states during scanning (Di et al., 2024b). The data revealed that even within a single individual, long-term correlations showed strong similarity with resting-state connectivity (ρ = 0.39).

However, it is important to note that neural activity measured across different temporal scales may not reflect identical processes. Thus, it remains unclear whether correlation structures derived from distinct temporal scales are directly comparable. Prior studies on fMRI time series have shown that connectivity structures within a single scanning session can vary depending on the frequency bands analyzed (Gohel and Biswal, 2015; Kajimura et al., 2023; Yuen et al., 2019). Future research could explore the comparison of correlation structures between slow and fast neural activity patterns to better understand their relationship.

Compared to earlier studies, the current research reports slightly higher correlations with resting-state connectivity. This improvement may stem from larger sample sizes, averaging data across multiple sessions, or advancements in the preprocessing pipeline. These findings imply that the smaller correlations observed in previous studies might partially result from noise, and that improvements in data acquisition and processing can enhance the observed similarities. Nonetheless, the analysis also highlights that each modality makes a unique contribution to the correlation structure, indicating an inherent limit to the similarities that can be achieved between different modalities.

This analysis validates the use of structural and functional brain measures to investigate interregional relationships, often referred to as functional connectivity when using functional data. Given the complex factors influencing these measures, controlling for certain variables can enhance the

interpretability of correlation results. Our findings demonstrated that intra-individual correlations, which account for individual differences, tend to exhibit stronger associations with resting-state functional connectivity compared to inter-individual correlations, supporting the value of such controls. However, it is important to note that multiple measures from the same individual are not always available, and in some cases, inter-individual correlations may be the only feasible approach.

5. Conclusion

The current results to some extent validated the usage of inter-individual correlations as an estimate of brain connectivity. The results also highlighted that multiple factors could contribute to the correlation structure. Those factors may need to control or taken care of to boost interpretability of the results.

Acknowledgement

This study was supported by grants from (US) National Institutes of Health for Xin Di (R15MH125332) and Bharat B. Biswal (5R01MH131335).
Data collection and sharing for this project was funded by the Alzheimer's Disease Neuroimaging Initiative (ADNI) (National Institutes of Health Grant U01 AG024904) and DOD ADNI (Department of Defense award number W81XWH-12-2-0012). ADNI is funded by the National Institute on Aging, the National Institute of Biomedical Imaging and Bioengineering, and through generous contributions from the following: AbbVie, Alzheimer's Association; Alzheimer's Drug Discovery Foundation; Araclon Biotech; BioClinica, Inc.; Biogen; Bristol-Myers Squibb Company; CereSpir, Inc.; Cogstate; Eisai Inc.; Elan Pharmaceuticals, Inc.; Eli Lilly and Company; EuroImmun; F. Hoffmann-La Roche Ltd and its affiliated company Genentech, Inc.; Fujirebio; GE Healthcare; IXICO Ltd.; Janssen Alzheimer Immunotherapy Research & Development, LLC.; Johnson & Johnson Pharmaceutical Research & Development LLC.; Lumosity; Lundbeck; Merck & Co., Inc.; Meso Scale Diagnostics, LLC.; NeuroRx Research; Neurotrack Technologies; Novartis Pharmaceuticals Corporation; Pfizer Inc.; Piramal Imaging; Servier; Takeda Pharmaceutical Company; and Transition Therapeutics. The Canadian Institutes of Health Research is providing funds to support ADNI clinical sites in Canada. Private sector contributions are facilitated by the Foundation for the National Institutes of Health (www.fnih.org). The grantee organization is the Northern California Institute for Research and Education, and the study is coordinated by the Alzheimer's Therapeutic Research Institute at the University of Southern California. ADNI data are disseminated by the Laboratory for Neuro Imaging at the University of Southern California.

References:

Alexander-Bloch, A., Giedd, J.N., Bullmore, E., 2013a. Imaging structural co-variance between human brain regions. Nat Rev Neurosci 14, 322–336. https://doi.org/10.1038/nrn3465

Alexander-Bloch, A., Raznahan, A., Bullmore, E., Giedd, J., 2013b. The convergence of maturational change and structural covariance in human cortical networks. The Journal of neuroscience : the official journal of the Society for Neuroscience 33, 2889–99. https://doi.org/10.1523/JNEUROSCI.3554-12.2013

Biswal, B., Yetkin, F.Z., Haughton, V.M., Hyde, J.S., 1995. Functional connectivity in the motor cortex of resting human brain using echo-planar MRI. Magnetic resonance in medicine : official journal of the Society of Magnetic Resonance in Medicine / Society of Magnetic Resonance in Medicine 34, 537–41. https://doi.org/10.1002/mrm.1910340409

Biswal, B.B., Mennes, M., Zuo, X.-N., Gohel, S., Kelly, C., Smith, S.M., Beckmann, C.F., Adelstein, J.S., Buckner, R.L., Colcombe, S., Dogonowski, A.-M., Ernst, M., Fair, D., Hampson, M., Hoptman, M.J., Hyde, J.S., Kiviniemi, V.J., Kötter, R., Li, S.-J., Lin, C.-P., Lowe, M.J., Mackay, C., Madden, D.J., Madsen, K.H., Margulies, D.S., Mayberg, H.S., McMahon, K., Monk, C.S., Mostofsky, S.H., Nagel, B.J., Pekar, J.J., Peltier, S.J., Petersen, S.E., Riedl, V., Rombouts, S.A.R.B., Rypma, B., Schlaggar, B.L., Schmidt, S., Seidler, R.D., Siegle, G.J., Sorg, C., Teng, G.-J., Veijola, J., Villringer, A., Walter, M., Wang, L., Weng, X.-C., Whitfield-Gabrieli, S., Williamson, P., Windischberger, C., Zang, Y.-F., Zhang, H.-Y., Castellanos, F.X., Milham, M.P., 2010. Toward discovery science of human brain function. Proceedings of the National Academy of Sciences of the United States of America 107, 4734–9. https://doi.org/10.1073/pnas.0911855107

Di, X., Biswal, and Alzheimer's Disease Neu, B.B., 2012. Metabolic Brain Covariant Networks as Revealed by FDG-PET with Reference to Resting-State fMRI Networks. Brain Connectivity 2, 275–283. https://doi.org/10.1089/brain.2012.0086

Di, X., Biswal, B.B., 2023. A functional MRI pre-processing and quality control protocol based on statistical parametric mapping (SPM) and MATLAB. Frontiers in Neuroimaging 1, 1070151.

Di, X., Gohel, S., Thielcke, A., Wehrl, H.F., Biswal, B.B., Alzheimer's Disease Neuroimaging Initiative, 2017. Do all roads lead to Rome? A comparison of brain networks derived from inter-subject volumetric and metabolic covariance and moment-to-moment hemodynamic correlations in old individuals. Brain structure & function 222, 3833–3845. https://doi.org/10.1007/s00429-017-1438-7

Di, X., Jain, P., Biswal, B.B., 2024a. Effects of Tasks on Functional Brain Connectivity Derived from Inter-Individual Correlations: Insights from Regional Homogeneity of Functional MRI Data. https://doi.org/10.1101/2024.06.02.597063

Di, X., Jain, P., Biswal, B.B., 2024b. Effects of Tasks on Functional Brain Connectivity Derived from Inter-Individual Correlations: Insights from Regional Homogeneity of Functional MRI Data. https://doi.org/10.1101/2024.06.02.597063

Duchesne, S., Dieumegarde, L., Chouinard, I., Farokhian, F., Badhwar, A., Bellec, P., Tétreault, P., Descoteaux, M., Boré, A., Houde, J.-C., Beaulieu, C., Potvin, O., 2019. Structural and functional multi-platform MRI series of a single human volunteer over more than fifteen years. Sci Data 6, 245. https://doi.org/10.1038/s41597-019-0262-8

Evans, A.C., 2013. Networks of anatomical covariance. NeuroImage 80, 489–504. https://doi.org/10.1016/j.neuroimage.2013.05.054

Fox, P.T., Raichle, M.E., 1984. Stimulus rate dependence of regional cerebral blood flow in human striate cortex, demonstrated by positron emission tomography. Journal of neurophysiology 51, 1109–20.

Gohel, S.R., Biswal, B.B., 2015. Functional Integration Between Brain Regions at Rest Occurs in Multiple-Frequency Bands. Brain Connectivity 5, 23–34. https://doi.org/10.1089/brain.2013.0210

Gong, G., He, Y., Chen, Z.J., Evans, A.C., 2012. Convergence and divergence of thickness correlations with diffusion connections across the human cerebral cortex. NeuroImage 59, 1239–1248. https://doi.org/10.1016/j.neuroimage.2011.08.017

He, Y., Chen, Z.J., Evans, A.C., 2007. Small-world anatomical networks in the human brain revealed by cortical thickness from MRI. Cerebral cortex (New York, N.Y. : 1991) 17, 2407–19. https://doi.org/10.1093/cercor/bhl149

Horwitz, B., Duara, R., Rapoport, S.I., 1984. Intercorrelations of Glucose Metabolic Rates Between Brain Regions: Application to Healthy Males in a State of Reduced Sensory Input. Journal of Cerebral Blood Flow & Metabolism 4, 484–499. https://doi.org/10.1038/jcbfm.1984.73

Kajimura, S., Margulies, D., Smallwood, J., 2023. Frequency-specific brain network architecture in resting-state fMRI. Sci Rep 13, 2964. https://doi.org/10.1038/s41598-023-29321-5

Lizarraga, A., Ripp, I., Sala, A., Shi, K., Düring, M., Koch, K., Yakushev, I., 2023. Similarity between structural and proxy estimates of brain connectivity. J Cereb Blood Flow Metab 0271678X231204769. https://doi.org/10.1177/0271678X231204769

Mechelli, A., Friston, K.J., Frackowiak, R.S., Price, C.J., 2005. Structural covariance in the human cortex. The Journal of neuroscience : the official journal of the Society for Neuroscience 25, 8303–10. https://doi.org/10.1523/JNEUROSCI.0357-05.2005

Metter, E.J., Riege, W.H., Kuhl, D.E., Phelps, M.E., 1984. Cerebral Metabolic Relationships for Selected Brain Regions in Healthy Adults. Journal of Cerebral Blood Flow & Metabolism 4, 1–7. https://doi.org/10.1038/jcbfm.1984.1

Phelps, M.E., Kuhl, D.E., Mazziota, J.C., 1981. Metabolic Mapping of the Brain's Response to Visual Stimulation: Studies in Humans. Science 211, 1445–1448. https://doi.org/10.1126/science.6970412

Schaefer, A., Kong, R., Gordon, E.M., Laumann, T.O., Zuo, X.-N., Holmes, A.J., Eickhoff, S.B., Yeo, B.T.T., 2018. Local-Global Parcellation of the Human Cerebral Cortex from Intrinsic Functional Connectivity MRI. Cerebral cortex (New York, N.Y. : 1991) 28, 3095–3114. https://doi.org/10.1093/cercor/bhx179

Song, X.-W., Dong, Z.-Y., Long, X.-Y., Li, S.-F., Zuo, X.-N., Zhu, C.-Z., He, Y., Yan, C.-G., Zang, Y.-F., 2011. REST: a toolkit for resting-state functional magnetic resonance imaging data processing. PloS one 6, e25031. https://doi.org/10.1371/journal.pone.0025031

Taylor, P.A., Gohel, S., Di, X., Walter, M., Biswal, B.B., 2012. Functional covariance networks: obtaining resting-state networks from intersubject variability. Brain connectivity 2, 203–17. https://doi.org/10.1089/brain.2012.0095

Tzourio-Mazoyer, N., Landeau, B., Papathanassiou, D., Crivello, F., Etard, O., Delcroix, N., Mazoyer, B., Joliot, M., 2002. Automated anatomical labeling of activations in SPM using a macroscopic anatomical parcellation of the MNI MRI single-subject brain. NeuroImage 15, 273–89. https://doi.org/10.1006/nimg.2001.0978

Vijayakumar, N., Ball, G., Seal, M.L., Mundy, L., Whittle, S., Silk, T., 2021. The development of structural covariance networks during the transition from childhood to adolescence. Sci Rep 11, 9451. https://doi.org/10.1038/s41598-021-88918-w

Yuen, N.H., Osachoff, N., Chen, J.J., 2019. Intrinsic Frequencies of the Resting-State fMRI Signal: The Frequency Dependence of Functional Connectivity and the Effect of Mode Mixing. Front Neurosci 13, 900. https://doi.org/10.3389/fnins.2019.00900

Zang, Y., Jiang, T., Lu, Y., He, Y., Tian, L., 2004. Regional homogeneity approach to fMRI data analysis. NeuroImage 22, 394–400. https://doi.org/10.1016/j.neuroimage.2003.12.030

Zang, Y.-F., He, Y., Zhu, C.-Z., Cao, Q.-J., Sui, M.-Q., Liang, M., Tian, L.-X., Jiang, T.-Z., Wang, Y.-F., 2007. Altered baseline brain activity in children with ADHD revealed by resting-state functional MRI. Brain & development 29, 83–91. https://doi.org/10.1016/j.braindev.2006.07.002

Zeki, S., Watson, J., Lueck, C., Friston, K., Kennard, C., Frackowiak, R., 1991. A direct demonstration of functional specialization in human visual cortex. J. Neurosci. 11, 641–649.

Zhang, Z., Liao, W., Zuo, X.-N., Wang, Z., Yuan, C., Jiao, Q., Chen, H., Biswal, B.B., Lu, G., Liu, Y., 2011. Resting-state brain organization revealed by functional covariance networks. PloS one 6, e28817. https://doi.org/10.1371/journal.pone.0028817